On the Statistical Relationship Between 90-Degree Configurations of Planetary Orbital Geometry and Solar Activity

Introduction

Our previous paper [1[1]] (Shaun: References will be added later) described a multi-element mechanism linking the orbital geometry of the solar system to fluctuations in collective investor sentiment. The mechanism consists of four elements:

1. **Solar Influence:** Planetary orbital geometry influences the stability of energy emission processes within the Sun.
2. **Ionospheric Coupling:** Modulations in solar emissions, specifically in low-frequency turbulence, affect the stability and altitude of the Earth's ionosphere.
3. **Wave Resonance:** Changes in ionospheric conditions alter the stability of global electromagnetic standing waves in the Earth-ionosphere cavity, known as Schumann resonances.
4. **Behavioral Modulation:** Shifts in the variability of these electromagnetic standing waves influence human neurophysiology and psychology, manifesting as changes in how responsive individuals are to negative and positive events and conditions. The simultaneous impact of these small forces on a large pool of individuals affects collective investor sentiment, which are subsequently reflected in stock market returns.

While Elements 2 and 3 are extrapolations from established ionospheric physics [6, 7], Elements 1 and 4 remain speculative. The purpose of our earlier paper was to describe a plausible causal pathway, present initial empirical evidence, and identify areas for further investigation.

The focus of this paper is on Element 1, and evaluates whether a specific planetary configuration is associated with measurable changes in short-term solar tranquility. We assess the statistical relationship between:

a. Changes in the stability of solar activity before, during, and after a specific planetary configuration (studies A and B)
b. The change in solar activity in the weeks after the end of the specific configuration (study C).

[1] https://papers.ssrn.com/sol3/papers.cfm?abstract_id=5482086

This paper. The analysis is empirical and does not attempt to specify the physical processes that may underlie this association. Such mechanisms are the subject of ongoing debate and are not required for the statistical results reported here.

Our studies use a metric of *solar tranquility* calculated from the SILO sunspot count. Solar tranquility is calculated as the sunspot count normalized to range from 0.0 to 1.0, with the scale is inverted (1-normalized value) to result in a measure of solar tranquility. The higher the value the more tranquil the Sun's surface is as indicated by the sunspot count. The SILO data was obtained from the GFZ.

The specific planetary configuration examined in this study is defined by a 90° angle between the geometric centers of two overlapping groups of planets. The first group comprises the inner and middle planets—Mercury through Saturn—and the second includes the outer planets, Jupiter through Neptune, with the Sun located at the vertex. In practice, this 90° configuration is defined as an angular range between 86° and 94°. This configuration appears to produce abrupt, self-contained shifts in both solar tranquility and patterns of market behavior. As described in (cite preprint) these configuration events coincide with stock market price inflection points encompassed in boom-and-bust patterns of performance.

The null hypothesis in all studies is that planetary configuration has no measurable impact on solar tranquility. Thus, any statistically significant results support the view that planets affect solar activity.

The underlying planetary coordinates were obtained from the NASA …more.

The timing of this paper is significant. Based on NASA data, the next cluster of 90-degree configuration events will begin in mid-2026 and end before 2027. Thus, 2026 will be a rare opportunity to verify, falsify, and refine in real time the relationships between the configuration events, electromagnetic standing waves, sunspot counts, and stock market performance.

2.2 Literature Context

The broader concept that solar and geomagnetic activity can influence human physiology and psychology has been explored in the literature. Studies have reported correlations between geomagnetic activity and rates of heart attacks, suicides, and mood disorders [8, 9]. More directly relevant to finance, Krivelyova and Robotti [10] found that stock returns tend to decline following periods of high geomagnetic activity, suggesting that geomagnetic disturbances may negatively affect investor mood and risk perception.

The relationship between planetary configuration and solar activity is more contentious. Although the prevailing view dismisses planetary gravitational and electromagnetic forces as too weak to materially affect the Sun [11], several studies have reported correlations between planetary alignments and solar cycle parameters [3, 4, 12]. The present study aligns with this minority perspective, proposing that planetary effects can induce a more laminar flow in the Sun's convective zone, for which sunspot counts serve as a practical, long-term proxy.

The potential influence of solar system dynamics on complex systems, including solar activity and human socio-economic behavior, represents a persistent and controversial topic in nonlinear science [1, 2]. While the mainstream view in solar physics holds that planetary gravitational influences are negligible, a body of research continues to investigate potential correlations [3, 4].

Several mechanisms have been proposed in the literature that link planetary geometry to solar variability, including tidal, resonant, and electromagnetic interactions. The present study does not attempt to evaluate these mechanisms. Our focus is solely on the statistical detection of a measurable response in solar tranquility associated with the 90-degree configuration.

The 90° Configuration of Two Planetary Groups

The specific planetary geometry we focus on is the angular separation between the centers of two overlapping planetary groups. The inner group consists of Mercury, Venus, Earth, Jupiter, Saturn. The outer group consists of Jupiter, Saturn, Uranus, Neptune. The 86-degree to 94-degree range allows analysis of a number of weeks close to the 90-degree mark. The four-degree span before and after the 90-degree mark was selected arbitrarily.

The calculated center of the inner planetary group is based on those planets' impact on shorter cycles of price acceleration of the stock market. The effects are sufficiently close to the standard formula for tidal forces ($F \propto M/d^3$) that we used the weights indicated by the tidal formula.

The calculated center of the outer group is based on those planets' impact on longer cycles of price acceleration of the stock market. Since such effects fall outside current views on physical effects, this approach is speculative. The final weights are presented in Table 1.

Table 1: Planetary Mass Weights for Orbital Group Centers

Planet	Weight in Inner Group	Weight in Outer Group
Mercury	14 %	—
Venus	34 %	—
Earth	15 %	—
Mars	—	—
Jupiter	35 %	35 %
Saturn	2 %	40 %
Uranus	—	12.5 %
Neptune	—	12.5 %
Total	100 %	100 %

Note: Weights used to calculate the center of mass for the inner (Mercury, Venus, Earth, Jupiter, Saturn) and outer (Jupiter, Saturn, Uranus, Neptune) planetary groups. The inner group center was calculated using standard tidal force proportionality (M/d^3). The outer group center was determined through an iterative optimization process to maximize correlations with long-term stock market price acceleration trends. The Sun is positioned at the vertex for angular measurements. Source: CPM Investing LLC calculations based on planetary mass and orbital data from NASA JPL Horizons.

The 90° configuration was initially identified through visual inspection of market data coinciding with the period before and after the 1987 stock market crash. The importance of the 90-degree configuration astrophysical studies of solar dynamics is described in Appendix L. We posit that

the two groups of planets exert electromagnetic and gravitational forces on the Sun. When at 90 degrees, these forces induce a more laminar flow in the Sun's convective zone. The outer planetary group, rather than exerting gravitational forces, acts to preserve the low frequency electromagnetic perturbations emanating from the Sun by its structure. This hypothesis is described in Appendix XX.

While we believe that the weighting scheme described above will create a reasonably accurate forecast for the 2026 cluster, the scheme should be refined in the future based on further research. The current scheme imparts a major role to Jupiter. A scheme that carves out Jupiter from each group and then describes the describes a three-point dynamic involving the inner planets, Jupiter, and the outer planets may be more explanatory. We believe that any inaccuracies of the current scheme would weaken the statistical results rather than strengthen them. Thus, the significance of the current findings support the validity of this scheme.

Since the focus of this paper is on the effect planets have on the Sun and human behavior, the specific nature of the weighting scheme is not crucial. Instead, the important condition for the analyses is that the scheme is constant over the 89-year period. For all tests, the null hypothesis is that planetary forces have no impact on the Sun or the Earth and its inhabitants. Any statistically significant finding will be worthy of further consideration and possibly deeper research.

Prior Analyses and Visual Evidence

To shed light on the possible relationship between planetary geometry and solar activity, this paper leverages the long-term sunspot record. Our primary hypothesis is that the 90° configuration introduces a more laminar flow within the Sun's convective zone, that results in less volatility low frequency electromagnetic perturbations emanating from the Sun. While we cannot measure the low frequency electromagnetic perturbations directly and data for the global electromagnetic standing waves is limited, sunspot activity is assumed to be a suitable proxy for determining if there is greater solar stability during the 90-degree configuration events over the 89-year period.

Visual evidence of the correlation between three 90-degree configuration events, our sunspot tranquility metric, and market performance from June 5, 2015 to December 31, 2019 is provided in Figure 1.

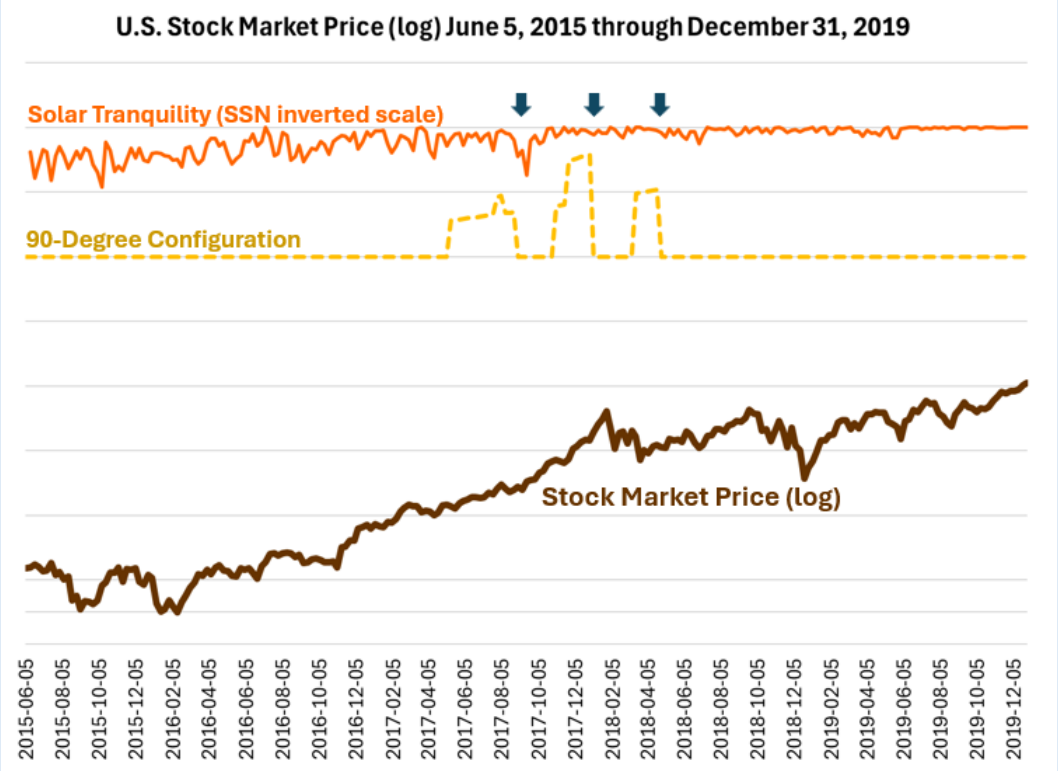

Fig. 1. Co-occurrence of market, solar, and planetary phenomena (2015-2021). The brown line shows the Dow Jones Industrial Average (DJIA). The orange line shows the solar tranquility metric (1 minus the normalized daily total sunspot number). Vertical gray bands indicate periods where the angular separation between the inner and outer planetary orbital centers was between 86° and 94°, as calculated from NASA JPL Horizons ephemeris data. Data sources: DJIA (MeasuringWorth); Sunspot Number (SILSO data/image, Royal Observatory of Belgium); Planetary Ephemerides (NASA JPL Horizons).

Figure 2 below shows the 89-year history of these series.

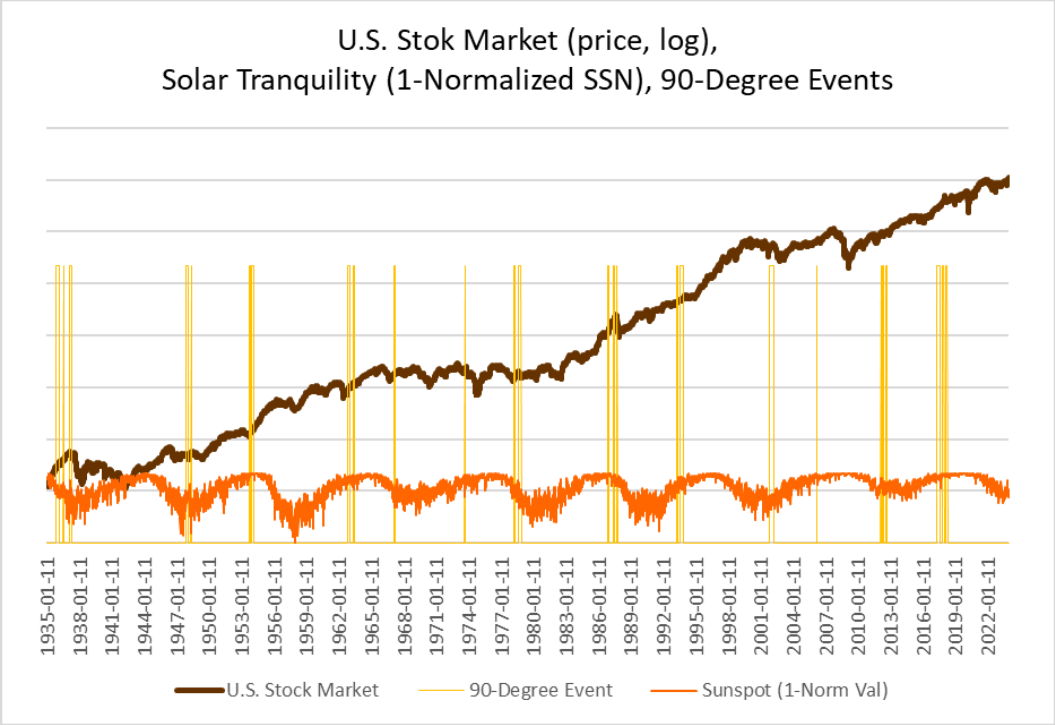

Fig. 2. Long-term context of 90° configuration clusters and U.S. stock market performance (1935-2024). tranquility metric (1 minus the normalized daily total sunspot number). Vertical gray bands indicate periods where the angular separation between the inner and outer planetary orbital centers was between 86° and 94°, as calculated from NASA JPL Horizons ephemeris data. Data sources: DJIA (MeasuringWorth); Sunspot Number (SILSO data/image, Royal Observatory of Belgium); Planetary Ephemerides (NASA JPL Horizons).

The solar tranquility series exhibits a well-documented ~11-year cycle driven by the Sun's internal dynamo. The 90° configurations are not phase-locked to this cycle, occurring at its peaks, troughs, and mid-phases, which suggests their influence is superimposed on the primary 11-year solar rhythm. The important point, however, is that our primary hypothesis does not involve sunspots directly over all periods because our testing indicated that sunspots and sunspot activity are not related extensively to investor sentiment.

We present the results of three studies of solar tranquility and the 26 90-degree configuration events.

Study A. Significantly More Stable Solar Tranquility During an Event Compared to the Prior 12 Weeks (Tab b and c)

This test focuses on the variability of the tranquility measure. Figure 3 shows three events in the 2017 cluster, and the pre-event, during-event, and post-event periods related to the three events.

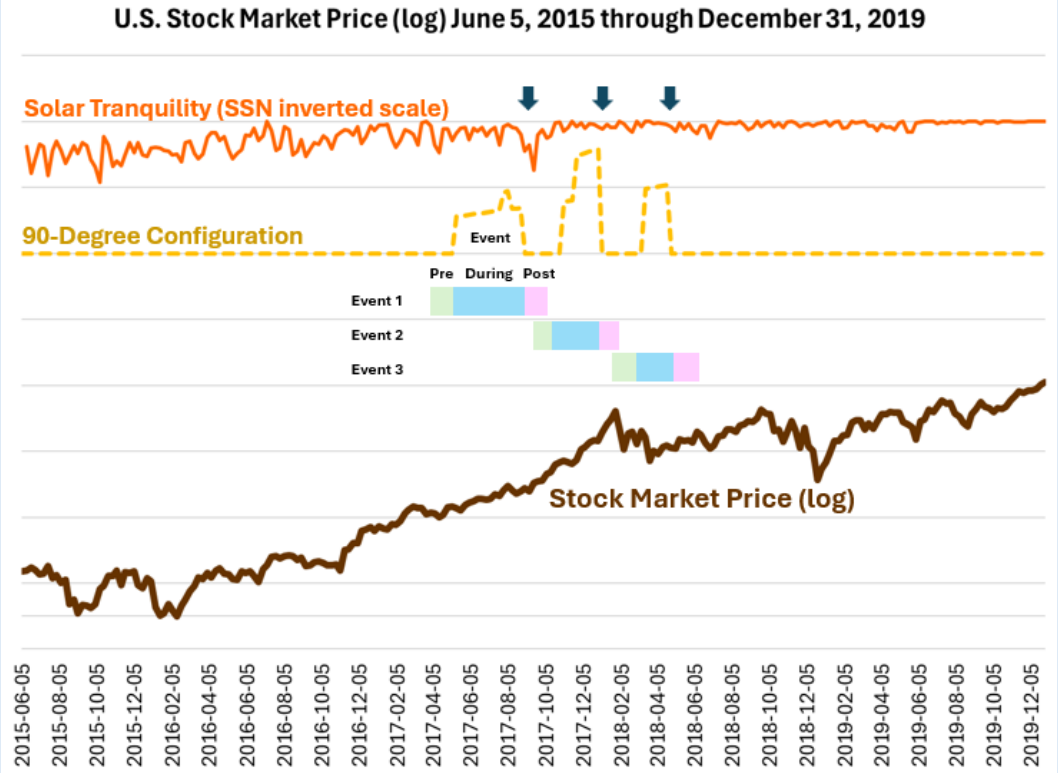

We evaluate the variability of solar tranquility during the three periods by creating two ratios.

1. Comparison of the pre-event period to the during period: Var(during)/Var(pre)
2. Comparison of the post-event period to the during period: Var(during)/Var(post)

If the 90-degre configurations have no impact on solar tranquility, we would expect ratios of 1.00 on average across the entire evaluation period. Results:

1. Across 26 90° configuration events, the median variance ratio Var(during)/Var(pre) was 0.56. The ratio is lower than the expected value of 1.0. Twenty-two of 26 events (85%) exhibited lower variance during the 90-degree event than in the twelve weeks preceding the event (one-sided binomial p = 0.0003). This proportion is highly significant.
2. Across 26 90° configuration events, the median variance ratio Var(during)/Var(post) was 0.71. Seventeen of 26 events (65%) showed lower variance during the 90-degree event than in the twelve weeks following the event (p = 0.084). This proportion does not meet the 0.05 threshold for statistical significance.

Stability of Solar Tranquility	26 Events	p-value
During vs Prior to Event		
Var(during) / Var(pre)	0.56	
Events with lower Var during	22 / 26 = 85%	0.0003
During vs After Event		
Var(during / Var(post)	71%	
Events with lower Var during	17 / 26 = 65%	0.0843

The lack of statistically significant effect after the 90-degree event may be related to a systematic drop in solar tranquility after the end of the 90-degree events. Drops in solar tranquility are indicated by the three arrows in Figure X above. We examine this pattern across all 26 events in Study B.

Study B. Reduced Sunspot Tranquility 4 weeks Following 90° Configurations (Tab d)

The analysis of solar tranquility revealed a non-random pattern following the end of 90° configurations. At the four-week horizon, the solar tranquility series moved lower (reflecting an increase in solar activity) in 77% of the post-event periods (20 out of 26 events). The probability of this occurring by chance, under the binomial distribution, is less than 1% ($p < 0.01$), allowing us to reject the null hypothesis of no effect. This four-week horizon showed the most pronounced effect across the 1- to 12-week horizons tested.

For context, in a random sample of 4,692 four-week periods across the entire dataset, 49.6% showed an increase and 50.4% a decrease, confirming the baseline randomness and highlighting the significance of the post-configuration signal.

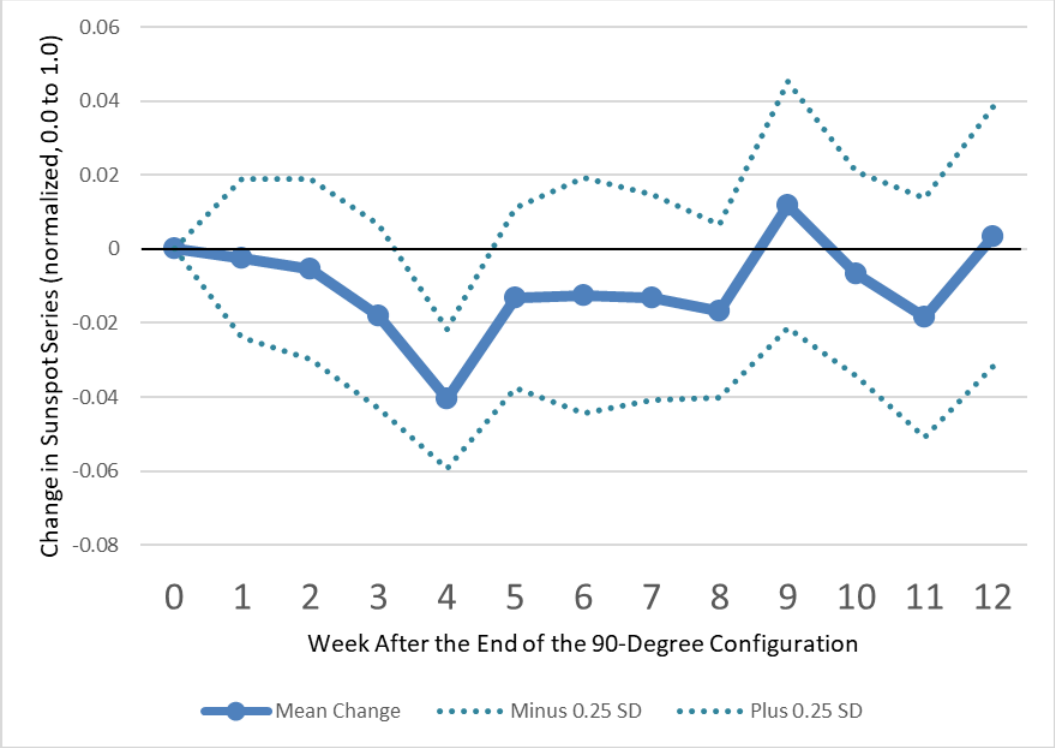

Fig. 3. Change in solar tranquility following 90° configuration events over horizons of 1 to 12 weeks following the end of each of the 26 individual 90° configuration events (1935-2023). The blue band represents ±1 standard error. The pronounced decline in solar tranquility (indicating an increase in solar activity) at the four-week horizon is statistically significant ($p < 0.01$, binomial test). Data sources: Sunspot Number (SILSO); Planetary Configurations (NASA JPL Horizons).

Table 3: Statistical Significance of Sunspot Series Changes Following 90° Configuration

Condition	Number of Periods	Percentage	p-value
Post-90° Config. (Decrease)	20 / 26	77%	< 0.01
All Random 4-Week Periods (Decrease)	2365 / 4692	50.4%	-

Note: Comparison of sunspot series directionality at the four-week horizon following 90° configuration events versus all possible four-week periods in the dataset (1935-2023). A "decrease" in the inverted series represents an increase in solar activity. The p-value is derived from a binomial test against the null hypothesis of a 50% probability of decrease. Source: CPM Investing LLC calculations using sunspot data from SILSO (Royal Observatory of Belgium) and planetary configuration data from NASA JPL Horizons.

Post Event Loss at 4 weeks	All 26 Events	p-value
Events with decline in solar tranquility at week 4 after an event	20 / 26 = 77%	0.0047

Study C evaluates the relationship between a measure of concentration of outer planets and the magnitude of the decline in solar tranquility four weeks after the end of the configuration event. The measure of planetary concentration is the distance between the Sun and the calculated center of the outer planetary group. Given the elliptical orbits of the planets, the greater this distance, the more spatially concentrated the members of the outer planetary group. Thus, the Sun-OuterCenter distance is a proxy for the concentration of the members of the outer group. The distance is normalized to range from 0.0 to 1.0, with the higher values indicating greater distance. This metric has been identified in prior studies as a factor contributing to the intensity of the change in investor sentiment.

Study C. The Greater the Distance Between the Sun and the Outer Group Center the Greater the Subsequent Decline in Solar Tranquility at Week +4 (Tab e)

The purpose of this study is to evaluate whether the post-event decline in solar tranquility is affected by the distance between the Sun and the center of the outer-planet group. The variables considered are:

1. The Sun-OuterCenter distance described above
2. The change in the level of solar tranquility four weeks after the end of the 90-degree configuration compared to the level at the end of the event. Negative values indicate that tranquility was lower at week 4 than at the event's end.

Across the twenty-six configurations in the 1935–2023 record, this four-week decrease was strongly associated with the Sun–Outer Center distance. Events that concluded when the outer-planet group's center was farther from the Sun showed systematically larger declines in tranquility. The relationship was moderate to strong in magnitude and statistically significant (Spearman $\rho \approx -0.57$, $p \approx 0.002$; standardized regression coefficient $\beta \approx -0.51$, $p \approx 0.009$). This result indicates that the Sun–Outer Center distance at the moment the configuration ends helps

determine the magnitude of the Sun’s short-term relaxation response after the 90-degree configuration event, with greater distance associated with a larger four-week reduction in tranquility.

The relationship between Sun-OuterCenter distance and the decrease at 4 weeks after the event was significant under both rank-based and linear measures (Spearman ρ = –0.57, p = 0.002; Pearson r = –0.52, p = 0.007), indicating a robust monotonic association between greater geometric separation and larger four-week reductions in tranquility.

Duration-4w Post Loss	All 26 Events	p-value
Spearman ρ	-0.57	0.002
Pearson r	-0.52	0.007

Discussion (early draft)

Within-Event Stability (±12 Weeks)

Across twenty-six 90° planetary configurations, the median variance ratio Var(during)/Var(pre) was 0.56, and Var(during)/Var(post) was 0.71. Twenty-two of 26 configurations (85%) exhibited lower variance during configurations than in the preceding twelve weeks (one-sided binomial $p = 0.0003$), while seventeen (65%) showed lower variance relative to the following twelve weeks ($p = 0.08$). The median within-event Spearman trend correlation was 0.65, indicating a consistent monotonic decline in true solar activity across configuration intervals when the inverted scale is considered. These results demonstrate that the stabilization effect persists across multiple solar rotations and provide strong statistical support for transient laminar flow within the Sun's convective zone during 90° configurations.

Transition to Market Response Analysis

If 90° configurations correspond to periods of enhanced laminar flow within the Sun's convective zone, the resulting reduction in solar variability should propagate outward through the heliosphere and influence the electromagnetic environment near Earth. The preceding analyses confirm that such stabilization occurs repeatedly and with statistical significance, implying that the Sun's convective dynamics—and thus its low-frequency energy output—are synchronized with specific planetary geometries. Within the broader framework, this laminarization phase should enhance ionospheric stability and the coherence of global electromagnetic standing waves. Because those standing waves interact with human neurophysiology, the stabilization of solar output could plausibly influence collective mood and decision-making.

If this interpretation is correct, aggregate investor sentiment should follow a predictable temporal pattern around each configuration cluster. Specifically, optimism and risk-taking should increase before and during clusters as solar conditions stabilize, leading to strong positive market returns and local price peaks within the cluster. As the configuration sequence ends and turbulence re-emerges, sentiment should reverse, producing sustained negative returns after the cluster.

Appendices

Appendix G –Solar Energy Metrics, Sources and Our Adjustments

This appendix describes the sources, transformation steps, and analytical roles of key solar energy metrics used in this study.

Sunspot Number (Inverted Scale)

The international sunspot number (SSN) is a standardized count of sunspot groups and individual spots on the solar surface. Higher values correspond to stronger solar magnetic activity and increased solar emissions. For this analysis, the SSN is inverted and normalized to align with market sentiment models, since periods of lower solar activity tend to coincide with higher investor confidence. Data are obtained from the Solar Influences Data Analysis Center (SILSO) and distributed by the GFZ German Research Centre for Geosciences. The GFZ sunspot number is the same as the International Sunspot Number (Rz), republished alongside long-term geomagnetic indices such as the aa and Ap indices (both of which measure variations in the Earth's magnetic field; the aa index extends back to 1868 and serves as a long-term proxy for solar wind activity), providing a uniform dataset widely used in solar–terrestrial research.

Orientation

Each of these solar metrics captures a distinct aspect of solar-terrestrial interaction. Inversion and normalization are used to align them with sentiment data. Except for the techniques mentioned above, we did not apply time lags to artificially enhance correlation with market sentiment.

Appendix L – The Role of Right-Angle Geometry in Astrophysics

The observation that Anxiety-Free Periods occur when the centers of inner and outer planetary orbits are separated by 90 degrees with the Sun at the vertex suggests that right-angle geometries may play a role in solar dynamics. While this specific application has not been previously proposed, astrophysical literature contains multiple contexts in which 90-degree angular relationships produce distinctive physical effects.

Polarization of Light at 90 Degrees: Rayleigh Scattering

Rayleigh scattering occurs when light interacts with particles that are much smaller than its wavelength, such as molecules in Earth's atmosphere. This scattering is stronger for shorter wavelengths, which is why the sky appears blue. Importantly, Rayleigh scattering is not only a change in the direction of light but also in its polarization (the orientation of the light waves). The degree of polarization depends on the angle between the incoming sunlight and the direction in which it is observed.

When this angle is 90 degrees, the polarization of the scattered light reaches its maximum. In practical terms, if one looks at a patch of the sky that is directly overhead when the Sun is on the horizon, the scattered light is highly polarized. This 90-degree geometry is routinely used in astrophysics and atmospheric physics to measure aerosols, detect planetary atmospheres, and study interstellar dust.[1]

This example demonstrates that orthogonal geometries (90 degrees) are not arbitrary but mark special points of physical significance in the behavior of electromagnetic radiation.

Tidal Forcing and Right-Angle Geometry

In celestial mechanics, the 90-degree separation of the Moon and Sun relative to Earth is known as quadrature. At this configuration, the tidal forces of the Sun and Moon act at right angles, partially cancelling one another. The result is a neap tide, a well-documented phenomenon where tidal range is minimized due to orthogonal force vectors.[2] This provides a clear example of how right-angle alignments reduce the coherence of otherwise reinforcing astrophysical forces.

Turbulence and Magnetic Field Orientation

In plasma astrophysics, turbulence and wave–particle interactions are strongly dependent on the angle between motion and magnetic fields. Energy transfer in solar wind turbulence is anisotropic, favoring directions perpendicular to the mean magnetic field. Perpendicular (near 90-degree) orientations can enhance nonlinear interactions, leading to altered transport and

---

[1] Coulson KL. Polarization and Intensity of Light in the Atmosphere. Hampton, VA: A. Deepak Publishing; 1988. NASA Technical Report Server entry available: https://ntrs.nasa.gov/citations/19880015415

[2] Cartwright DE, Tayler RJ. New computations of the tide-generating potential. Geophys J R Astron Soc. 1971;23(1):45–74. https://doi.org/doi:10.1111/j.1365-246X.1971.tb01803.x

dissipation of energy.[3] [4] Similarly, cyclotron resonance occurs when charged particles interact with electromagnetic waves at pitch angles near 90 degrees, a geometry that maximizes wave–particle coupling in some regimes.[5]

Dynamo Symmetry and Orthogonal Forcing

The solar dynamo, which underlies sunspot formation, is highly sensitive to changes in boundary conditions and symmetry breaking. External gravitational or electromagnetic influences that act at right angles to existing field structures may perturb the coherence of the dynamo in ways that differ qualitatively from in-line alignments (0° or 180°). Although direct evidence is limited, models of magnetic field evolution emphasize the role of symmetry and angular orientation in maintaining or disrupting coherent magnetic structures.[6]

Relevance to Anxiety-Free Periods

Taken together, these examples highlight that right-angle geometries are not neutral but often associated with reduced coherence, enhanced cross-field interaction, or distinct dynamical states. By analogy, when the inner and outer orbital centers form a 90-degree angle with the Sun, the orthogonal geometry may act to redistribute or dampen turbulence in the solar wind. Such changes could propagate into the solar dynamo, manifesting as altered sunspot numbers. This interpretation provides a physics-based framework linking orbital geometry to solar variability, consistent with the empirical correlation of AFPs and sunspot changes.

[3] Tu C, Marsch E. MHD structures, waves and turbulence in the solar wind: observations and theories. Space Sci Rev. 1995;73(1-2):1-210.
[4] Bruno R, Carbone V. The solar wind as a turbulence laboratory. Living Rev Sol Phys. 2013;10(1):2. https://doi.org/10.12942/lrsp-2013-2
[5] Smith CW, Hamilton K, Vasquez BJ, Leamon RJ. Dependence of the dissipation range spectrum of interplanetary magnetic fluctuations on the rate of energy cascade. Astrophys J Lett. 2006;645(1):L85-8.
[6] Charbonneau P. Dynamo models of the solar cycle. Living Rev Sol Phys. 2010;7(3). https://doi.org/10.12942/lrsp-2010-3

Appendix K – Emission Preservation Zone

We propose that when the magnetic environments of the outer planets—Jupiter, Saturn, Uranus, and Neptune—are clustered within a confined sector of the solar system, they contribute to the preservation of low-frequency electromagnetic emissions. In such a configuration, the overlapping planetary magnetospheres create an Emission Preservation Zone between the Sun and the cluster. This zone reduces the usual damping and scattering of extremely low-frequency perturbations, allowing them to remain coherent over greater distances and reach Earth more intact.

Introduction

The heliosphere contains a spectrum of electromagnetic and plasma (magnetohydrodynamic, or MHD) fluctuations generated by solar activity. As these disturbances travel outward, small high-frequency ripples typically dissipate quickly through nonlinear cascade and heating. In contrast, large-scale, low-frequency fluctuations are more resilient and can persist well beyond the orbit of Saturn, more than ten astronomical units from the Sun.[7]

These low-frequency waves are particularly sensitive to large-scale plasma and magnetic structures. Unlike high-frequency radiation such as X-rays, which travels through the heliosphere largely unaffected, extremely low-frequency waves (below ~100 Hz) interact with the charged plasma environment. Their survival depends on the structure of the interplanetary medium they traverse.[8] [9]

Emission Preservation Zone

When Jupiter, Saturn, Uranus, and Neptune cluster together, their combined magnetic fields may form a structured pathway in space. This environment can preserve extremely low-frequency perturbations by reducing phase distortion and scattering, enabling them to propagate coherently over long distances. The effect is not amplification but conservation: solar-origin signals that would normally decay before reaching Earth remain measurable at 1 AU.

By contrast, when the outer planets are more widely dispersed, the guiding effect weakens. In such periods, emissions scatter more readily, lose coherence, and dissipate before reaching Earth. This implies a geometry-dependent preservation of emissions: coherence is enhanced during clustering and diminished during dispersion.

---

[7] Richardson JD, Paularena KI, Lazarus AJ, Belcher JW. Radial evolution of the solar wind from IMP 8 to Voyager 2. Adv Space Res. 1996;18(1–2):17–26.

[8] Tu C, Marsch E. MHD structures, waves and turbulence in the solar wind: observations and theories. Space Sci Rev. 1995;73(1-2):1-210.

[9] Goldstein ML, Roberts DA, Matthaeus WH. Magnetohydrodynamic turbulence in the solar wind. Annu Rev Astron Astrophys. 1995;33:283-325.
https://doi.org/10.1146/annurev.aa.33.090195.001435

An Antipodal Region of Greater Damping

This hypothesis also suggests a corresponding antipodal region—opposite the planetary cluster—where no such preservation occurs. In this sector, the absence of organized magnetic structures increases damping and scattering, producing a more chaotic propagation environment.

Magnetic Field Topology and Planetary Differences

Jupiter and Saturn possess strong, largely dipolar magnetic fields aligned with their rotation axes. These stable magnetospheres, along with structures such as Jupiter's Io plasma torus, inject plasma and support extended magnetotails that interact persistently with the solar wind.[10] By contrast, Uranus and Neptune display highly tilted, multipolar magnetic fields that vary in orientation and coupling with the solar wind.[11] [12] Voyager observations confirm that these environments are sources of localized turbulence and wave activity. When clustered, the combined influence of these diverse magnetospheres may reinforce the preservation of solar-origin low-frequency perturbations.

Analogies and Modeling Considerations

The Emission Preservation Zone can be likened to acoustic resonance in cathedrals, where architectural geometry sustains sound waves instead of damping them.[13] In electromagnetic terms, it is similar to a waveguide or resonant cavity, where constructive interactions with boundary conditions allow certain frequencies to persist.[14] These analogies highlight how geometry and structure can sustain energy transmission without amplification.

From a modeling standpoint, the outer planets should be treated as dynamic, spatially extended magnetic scatterers. Global MHD simulations that incorporate realistic planetary field geometries and heliospheric turbulence may clarify how clustering configurations alter the propagation of low-frequency waves.

Empirical Support

Our Study B shows that during outer-planet clustering, correlations among weekly solar activity indicators—including the Sunspot Number, Ap Index, and F10.7 flux—are elevated. This suggests that the interplanetary medium may offer less distortion in such periods. The Oulu Neutron Monitor, while not a direct measure of solar wind turbulence, also shows increased

---

[10] Thomas N, Bagenal F, Hill T, Wilson J. The Io neutral clouds and plasma torus. In: Bagenal F, Dowling TE, McKinnon WB, editors. Jupiter: The Planet, Satellites and Magnetosphere. Cambridge University Press; 2004. p. 561–591.

[11] Ness NF, Acuña MH, Burlaga LF, et al. Magnetic field observations near Uranus: Voyager 2 results. Science. 1986;233(4759):85–89.

[12] Connerney JEP, Acuña MH, Ness NF. The magnetic field of Neptune. J Geophys Res. 1991;96(S01):19023–19042.

[13] Blesser B. An acoustical interpretation of classical architecture. J Acoust Soc Am. 2001;109(6):2972.

[14] Howes GG, Dorland W, Cowley SC, Hammett GW, Quataert E, Schekochihin AA, Tatsuno T. A model of turbulence in magnetized plasmas: implications for the dissipation range in the solar wind. J Geophys Res. 2008;113:A05103.
https://doi.org/10.1029/2007JA012665

coherence with solar indicators, consistent with changes in heliospheric structure during clustering episodes.

Limitations and Uncertainties

Uncertainties remain in this hypothesis. While magnetospheres clearly shape local plasma structures, their collective effect across interplanetary distances has not been directly observed. Disentangling planetary effects from solar cycle variability poses challenges. The precise angular span defining a clustered state requires refinement, and global simulations capable of integrating planetary magnetospheres with heliospheric turbulence are still in development.

Appendix: Statistical Verification and Replication Notes

A1. Data and Metrics

The analyses used two independent datasets:

1. **Solar Stability Metric** – the inverse of weekly sunspot number (SIDC dataset), representing greater stability when values increase.
    - Variance calculated for pre-, during-, and post-configuration periods.
    - 90° configuration dates derived from planetary orbital centers computed using NASA JPL ephemerides (Mercury–Neptune).
2. **Market Performance Metric** – weekly log returns of the Dow Jones Industrial Average (DJIA), 1933–2024.
    - Configuration clusters defined using the same orbital geometry windows as the solar dataset.

All calculations can be replicated using any spreadsheet or statistical package capable of computing variance, correlation, and binomial probabilities.

A2. Variance Ratio Tests (Solar and Market Stability)

For each configuration *i*, variances were calculated for weekly data during the 12-week pre-, during-, and post-configuration intervals.

$$R_{1,i}=\frac{Var(during_i)}{Var(pre_i)}, R_{2,i}=\frac{Var(during_i)}{Var(post_i)}$$

Median ratios summarize the central tendency across all 26 configurations.

To assess whether variance decreased during configurations, a one-sided binomial test was used:

$$p=\sum_{k=x}^{n}\binom{n}{k}(0.5)^k(0.5)^{n-k}$$

where

- x = number of configurations with ratio < 1,
- n = total configurations (26).

Excel equivalent:

```
=1-BINOM.DIST(x-1, n, 0.5, TRUE)
```

For example, with $x = 22$ and $n = 26$,
$p = 0.0003$, confirming statistically significant stabilization.

A3. Pre- and Post-Peak Return Test (Market Sentiment Phase)

Each configuration cluster was analyzed for pre-peak and post-peak performance:

$$Gain_i = \frac{P_{peak,i} - P_{low,pre,i}}{P_{low,pre,i}}, Loss_i = \frac{P_{low,post,i} - P_{peak,i}}{P_{peak,i}}$$

Median Gain = 6.5%, Median Loss = –2.1%.

Directional consistency was tested using the one-sided binomial test:

$$p = 1 - \underset{DIST}{\cdot}(k-1, n, 0.25, TRUE)$$

where $k = 25$ configurations with (Gain > 0, Loss < 0).
The 0.25 expectation reflects random market direction (0.5 × 0.5).
Result: $p \approx 0.000004$, rejecting the null hypothesis of randomness.

A4. Trend Correlation (Solar Variance)

For each configuration, the Spearman rank correlation between week number and solar stability metric during the event was computed:

$$\rho_i = cor(rank_t, rank_y)$$

Median $\rho = 0.65$, indicating a monotonic increase in stability (decrease in true sunspot activity) within 90° configurations.

Appendix X. Standardized Market Displacement During 90° Planetary Configurations

To evaluate the magnitude of market displacements associated with the 90° planetary configurations described in the main text, we standardized each configuration's cumulative price change relative to the long-term behavior of the Dow Jones Industrial Average (DJIA). Weekly DJIA data from 1935–2024 were expressed as logarithmic returns

$$\rho_t = \ln\left(\frac{P_t}{P_{t-1}}\right),$$

where P_t is the weekly closing price. Logarithmic returns are additive across time and approximately normally distributed for large samples, providing a suitable baseline for multi-week aggregation.

The mean and standard deviation of weekly log returns were estimated from the full period (excluding the 90° configuration intervals):

$$\mu = 0.00127, \sigma = 0.02168.$$

For each configuration i of duration n_i weeks, the cumulative log return was calculated as

$$\rho_i = \sum_{t=1}^{n_i} \rho_t = \ln\left(\frac{P_{\text{end},i}}{P_{\text{start},i}}\right),$$

and the corresponding standardized deviation (z-score) as

$$z_i = \frac{\rho_i - n_i \mu}{\sqrt{n_i}\sigma}.$$

Positive z_i values indicate cumulative gains greater than expected under the background DJIA distribution, while negative values indicate unusually weak or declining periods. This normalization removes differences in window length and expresses each configuration's total return in units of the DJIA's typical week-to-week variability.

Across the thirteen identified 90° configurations, pre-configuration windows show a mean $z \approx +1.3$, whereas post-configuration windows show a mean $z \approx -1.9$. Several individual configurations exceed $|z| > 2$, including 1937 and 1987, indicating cumulative market movements beyond the 95 % range of background volatility. These standardized deviations confirm that the 90° configurations coincide with statistically exceptional phases of market behavior—periods of abnormally high pre-peak appreciation followed by unusually rapid declines.

Although the z-scores are not intended as formal inferential tests, they provide a scale-free measure of market displacement relative to the DJIA's intrinsic noise level. In this sense, the z-scores support the interpretation that the 90° planetary configurations mark boundary conditions in the long-term sentiment dynamics described in the main text: intervals during which market behavior departs from equilibrium expectations by multiple standard deviations in a direction consistent with the predicted laminar-to-turbulent transition in solar-driven investor sentiment.

Appendix B. Confidence Bounds for Joint Probability Estimates (not Used)

To evaluate the likelihood that the return patterns observed during 90-degree event clusters could arise by chance, we calculated the empirical probabilities P_{pre} and P_{post} for each event. These represent, respectively, the frequency with which a comparable pre-peak rise and post-peak decline occurred elsewhere in the 1933–2023 Dow Jones Industrial Average record, within ±1 week and ±1 % of the observed values. The product of these two frequencies gives the joint probability**:**

$$P_{\text{joint}} = P_{\text{pre}} \times P_{\text{post}},$$

which approximates the chance of observing both the pre- and post-peak dynamics in the same episode under an assumption of independence.

Because most probabilities were extremely small (typically well below 1 %), conventional normal approximations can understate uncertainty. To ensure robustness, two complementary methods were applied to derive 95 % confidence intervals for each joint probability:

1. **Delta-Method Confidence Interval (Primary).**
   The variance of the joint probability was estimated as

   $$Var\left(P_{\text{joint}}\right) \approx P_{\text{post}}^2 \; Var\left(P_{\text{pre}}\right) + P_{\text{pre}}^2 \; Var\left(P_{\text{post}}\right),$$

   with $Var\left(P_i\right) \approx P_i\left(1 - P_i\right)/n_i$ for each proportion computed from n_i candidate windows. The 95 % confidence interval was then

   $$P_{\text{joint}} \pm 1.96 \; \sqrt{Var\left(P_{\text{joint}}\right)}.$$

   This method provides a symmetric, analytic estimate suitable for small probabilities derived from large sample counts.

2. **Conservative Product-of-Bounds Interval (Robustness Check).**
   Each individual proportion (P_{pre}, P_{post}) was first assigned a Wilson score interval, which offers accurate coverage even for small or rare proportions. The joint bounds were then computed as

   $$\text{Lower} = L_{\text{pre}} \times L_{\text{post}}, \text{Upper} = U_{\text{pre}} \times U_{\text{post}}.$$

   This formulation is deliberately conservative: it assumes positive dependence between the two probabilities and produces slightly wider intervals than the delta-method.

Both approaches yielded consistent results, and the confidence bounds remained several orders of magnitude below 1 %. Even under the conservative formulation, no Anxiety-Free Period displayed a joint probability exceeding 0.01.

These findings reinforce the central conclusion that the pre- and post-peak return structures characteristic of 90-degree event clusters are statistically rare and highly non-random within the historical market record. They represent patterns unlikely to occur by chance, consistent with the hypothesis that clusters timing is governed by physical, rather than purely stochastic, drivers.

Footnote

Although the pre- and post-peak portions of an Anxiety-Free Period occur consecutively, the assumption of statistical independence between $P_{\text{pre}}$and P_{post}provides a conservative and tractable approximation. The pre-peak advance reflects the buildup of optimism during a rising phase, while the post-peak decline reflects its dissipation under changing sentiment and market conditions. These processes arise from different behavioral and physical dynamics and can therefore be treated as effectively independent for probability estimation. Empirically, weekly return autocorrelation in the Dow Jones Industrial Average is close to zero, supporting the assumption that adjacent return segments can be regarded as independent. Any residual correlation would likely reduce, rather than increase, the chance of observing both extreme outcomes in sequence, making the joint probabilities reported here conservative.

Appendix U – Data Sources

The datasets used in this report span solar, geomagnetic, financial, and cosmic ray domains. They were selected for their continuity, scientific credibility, and relevance to understanding heliospheric conditions and investor sentiment.

Solar and geomagnetic indices

Royal Observatory of Belgium. International Sunspot Number (Version 2). Brussels: SILSO, World Data Center Sunspot Index and Long-term Solar Observations; 2025.
https://www.sidc.be/silso/datafiles.

Financial market and economic data

U.S. Bureau of Economic Analysis. National Income and Product Accounts. Washington (DC): BEA; 2025.
https://www.bea.gov/data/economy/national;
MeasuringWorth. Dow Jones Industrial Average, daily, monthly, and annual data, 1896–present; 2025.
https://www.measuringworth.com/datasets/DJA/

Figures show normalized or transformed representations of performance; raw index levels are not reproduced. All financial data are used solely for research purposes and are not redistributed commercially.